

Distributed Training of Large Graph Neural Networks with Variable Communication Rates

Juan Cerviño*, Md Asadullah Turja*, Hesham Mostafa*, Nageen Himayat, Alejandro Ribeiro

Abstract—Training Graph Neural Networks (GNNs) on large graphs presents unique challenges due to the large memory and computing requirements. Distributed GNN training, where the graph is partitioned across multiple machines, is a common approach to training GNNs on large graphs. However, as the graph cannot generally be decomposed into small non-interacting components, data communication between the training machines quickly limits training speeds. Compressing the communicated node activations by a fixed amount improves the training speeds, but lowers the accuracy of the trained GNN. In this paper, we introduce a variable compression scheme for reducing the communication volume in distributed GNN training without compromising the accuracy of the learned model. Based on our theoretical analysis, we derive a variable compression method that converges to a solution equivalent to the full communication case, for all graph partitioning schemes. Our empirical results show that our method attains a comparable performance to the one obtained with full communication. We outperform full communication at any fixed compression ratio for any communication budget.

Index Terms—Graph Neural Networks, Distributed Training.

I. INTRODUCTION

GRAPH Neural Networks (GNNs) are a neural network architecture tailored for graph-structured data [1]–[3]. GNNs are multi-layered networks, where each layer is composed of a (graph) convolution and a point-wise non-linearity [4]. GNNs have shown state-of-the-art performance in robotics [5], [6], weather prediction [7], protein interactions [8] and physical system interactions [9], to name a few. The success of GNNs can be attributed to some of their theoretical properties such as generalization [10], [11], being permutation-invariant [12], [13], stable to perturbations of the graph [14], transferable across graphs of different sizes [15], and their expressive power [16]–[19].

In a GNN, the data is propagated through the graph via graph convolutions, which aggregate information across neighborhoods. In large-scale graphs, the data diffusion over the graph is costly in terms of computing and memory requirements. To overcome this limitation, several solutions were proposed. Some works have focused on the transferability properties of GNNs, i.e. training a GNN on a small graph and deploying it on a large-scale graph [15], [20]. Other works have focused on training on a sequence of growing graphs [21], [22]. Though useful, these solutions either assume

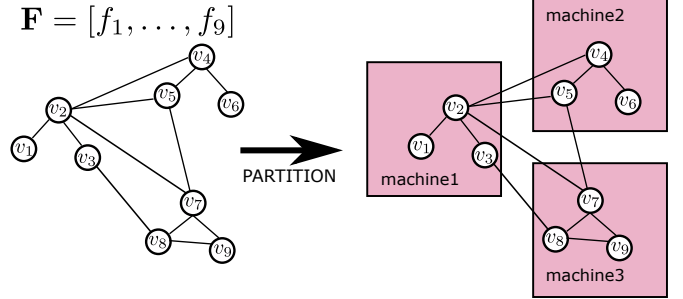


Fig. 1: Example of partitioning a graph with 9 nodes into 3 machines. Each machine only stores the features of the nodes in their corresponding partition.

that an accuracy degradation is admissible (i.e. transferability bounds), or that all the graph data is readily accessible within the same training machine. These assumptions may not hold in practice, as we might need to recover the full centralized performance without having the data in a centralized manner.

Real-world large-scale graph data typically cannot fit within the memory of a single machine or accelerator, which forces GNNs to be learned in a distributed manner [23]–[26]. To do this efficiently, several solutions have been proposed. There are *data-parallel* approaches that distribute the data across different machines where model parameters are updated with local data and then aggregated via a parameter server. Another solution is *federated learning* (FL), where the situation is even more complex as data is naturally distributed across nodes and cannot be shared to a central location due to privacy or communication constraints [27]–[29]. Compared to data parallel approaches FL suffers from data heterogeneity challenges as we cannot control the distribution of data across nodes to be identically distributed [30]. The GNN-FL adds additional complexity as the graph itself (input part of the model) is split across different machines. The GNN-FL counterpart has proven to be successful when the graph can be split into different machines [31], [32]. However, training locally while assuming no interaction between datasets is not always a reasonable assumption for graph data.

Two observations of GNNs draw this work. First, large graph datasets cannot be split into non-interacting pieces across a set of machines. Therefore, training GNNs distributively requires interaction between agents in the computation of the gradient updates. Second, the amount of communicated data affects the performance of the trained model; the more we communicate the more accurate the learned model will be. In this paper, we posit that the compression rate in

*These authors contributed equally to the paper. JC, AR are with the Department of Electrical and Systems Engineering, University of Pennsylvania, PA. MAT is with the University of North Carolina at Chapel Hill. HM, NH are with the Intel Corporation. JC is the corresponding author jcevino@seas.upenn.edu.

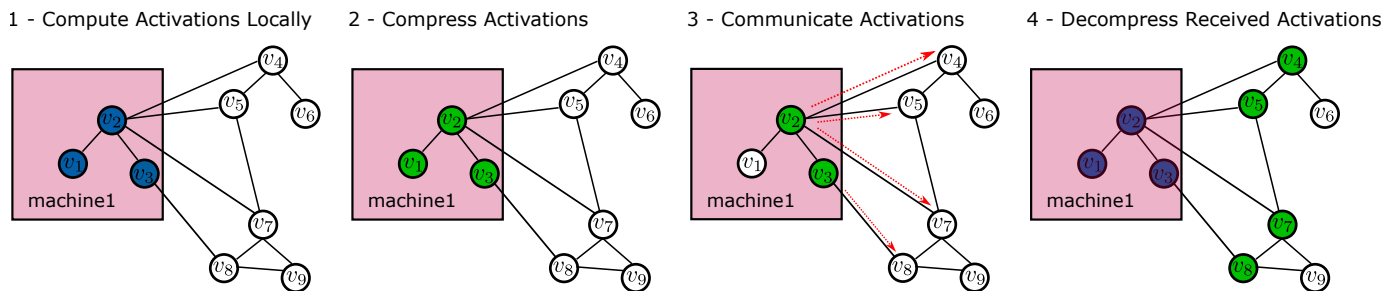


Fig. 2: To compute a gradient step, we need to gather the data. To do so, each machine starts by **computing** the activations of the local nodes. Then, these activations are **compressed** and **communicated** to adjacent machines. Once all the activations are communicated, each machine **decompresses** the data from the compressed nodes.

the communication between agents should vary between the different stages of the GNN training. Intuitively, at the early stages of training, the communication can be less reliable, but as training progresses, and we are required to estimate the gradient more precisely, the quality of the communicated data should improve. This observation translates into a varying compression rate, that compresses more at the early stages of training, and less at the later ones.

This paper considers the problem of efficiently learning a GNN across a set of machines, each of which has access to part of the graph data (see Figure 1). Drawn from the observation that in a GNN, model parameters are significantly smaller than the graph’s input and intermediate node feature, we propose to compress the intermediate GNN node features that are communicated between different machines. Given that this compression affects the accuracy of the GNN, in this paper we introduce a variable compression scheme that trades off the communication overhead needed to train a GNN distributively and the accuracy of the GNN.

The contributions of this paper are:

- 1) We present a novel algorithm to learn graph representations while compressing the data communicated between the training agents. We propose to vary the compression rate progressively, to achieve a comparable performance to the no-compression case at a fraction of the communication cost.
- 2) We present a method that does not require a specific graph partitioning setup, allowing it to be used when the graph partitioning cannot be controlled. We validate this thrust empirically by training on random graph partitioning.
- 3) We theoretically show that our method converges to a first-order stationary point of the full graph training problem while taking distributed steps and compressing the inter-server communications.
- 4) We empirically show that our method attains a comparable performance to the full communication training scenario while incurring fewer communication costs. In particular, by plotting accuracy as a function of the communication costs, our method outperforms full communication and fixed compression rates in terms of accuracy achieved per communicated byte.

RELATED WORK

Mini-Batch Training. In the context of distributed GNN training, [25] proposes to distribute mini-batches between a set of machines, each of which computes a local gradient, updates the GNN, and communicates it back to the server. [25] uses METIS [33] to partition the graph, which reduces communication overhead and balances the computations between machines. Although [25] provides good results in practice, the GNN does not process data on the full graph, only a partition of it, which can yield sub-optimal results compared to processing the full graph. In [34] they employ a policy to cache data associated with frequently accessed vertices in remote partitions. This method reduces the communications across partitions by creating local copies of the data.

Memory Optimization. In this work we do full batch training, which has also been considered in the literature. Similar to us is *sequential aggregation and rematerialization* [35], which sequentially re-constructs and frees pieces of the large GNN during the backward pass computation. Even in densely connected graphs, this deals with the memory limitations of the GNN, showing that the memory requirements per worker decrease linearly with the number of workers. Others have studied similar approaches in the context of distributed training [36]. In [37] they propose to use a balanced partitioning of the graph, as well as a shared memory implementation. They utilize a delayed partial aggregation of remote partitions by either ignoring or delaying feature vector aggregation during training.

Quantization. A related approach to dealing with the limitations of a single server for training compression in communication is quantization in the architecture. To train GNNs more efficiently using quantization, the most salient examples are feature quantization [38], Binary Graph Neural Networks [39], vector quantization [40], last bit quantization [41], and degree quantization [42]. There are also works on adaptive quantization of the messages between machines. In [43], they adapt the quantization level using stochastic integer quantization. However similar, this work adapts the quantization level locally, at the message level, which differs from our global view of compression. In all, although related in spirit, quantizing a GNN is a local operation that differs from compressing the communication between servers.

Sampling Based Methods Our method can be applied in

conjunction with sampling-based methods. In sampling-based methods, each node only aggregates from a random subset of its neighbors [44]–[47]. In the context of distributed learning, this random subset could include remote nodes. Therefore communication between machines becomes a bottleneck, and our method would still be relevant to reduce the communication volume. If we bias the sampling to only consider local nodes, then this would hurt performance, as it is equivalent to splitting the graph into multiple disconnected components, which does not work well in practice.

II. LEARNING GRAPH NEURAL NETWORKS

In this paper, we consider the problem of training GNNs on graphs that are stored in a set of machines. Formally, a graph is described by a set of vertices and edges $\mathcal{G} = (\mathbf{V}, \mathbf{E})$, where $|\mathbf{V}| = n$ is the set of vertices whose cardinality is equal to the number of nodes n , and $\mathbf{E} \subseteq \mathbf{V} \times \mathbf{V}$ is the set of edges. The graph \mathcal{G} can be represented by its adjacency matrix $\mathbf{S} \in \mathbb{R}^{n \times n}$. Oftentimes, the graph includes vertex features, $F_V \in \mathbb{R}^{|\mathbf{V}| \times |D_v|}$, and edge features, $F_E \in \mathbb{R}^{|\mathbf{E}| \times |D_e|}$, where D_v and D_e are the vertex and edge feature dimensions, respectively. Graph problems fall into three main categories: node-level prediction where the goal is to predict properties of individual nodes; edge-level prediction where the goal is to predict edge features or predict the locations of missing edges; and graph-level prediction where the goal is to predict properties of entire graphs. In this paper, we focus on distributed training of GNNs for node classification problems. Our distributed training approach is still relevant to the other two types of graph problems, as they also involve a series of GNN layers, followed by readout modules for edge-level or graph-level tasks.

A GNN is a multi-layer architecture, where at each layer, messages are aggregated between neighboring nodes via graph convolutions. Formally, given a graph signal $\mathbf{x} \in \mathbb{R}^n$, where $[\mathbf{x}]_i$ represents the value of the signal at node i , the graph convolution can be expressed as

$$\mathbf{z}_n = \sum_{k=0}^{K-1} h_k \mathbf{S}^k x_n, \quad (1)$$

where $\mathbf{h} = [h_0, \dots, h_{K-1}] \in \mathbb{R}^K$ are the graph convolutional coefficients. In the case that $K = 2$, and \mathbf{S} is binary, the graph convolution (1) translates into the AGGREGATE function in the so-called *message-passing neural networks*. A GNN is composed of L layers, each of which is composed of a graph convolution (1) followed by a point-wise non-linear activation function ρ such as ReLU, or \tanh . The l -th layer of a GNN can be expressed as,

$$\mathbf{X}_l = \rho \left(\sum_{k=0}^{K-1} \mathbf{S}^k \mathbf{X}_{l-1} \mathbf{H}_{l,k} \right), \quad (2)$$

where $\mathbf{X}_{l-1} \in \mathbb{R}^{n \times F_{l-1}}$ is the output of the previous layer (with \mathbf{X}_0 is equal to the input data $\mathbf{X} = [\mathbf{x}_1, \dots, \mathbf{x}_n] \in \mathbb{R}^{n \times F_0}$), and $\mathbf{H}_{l,k} \in \mathbb{R}^{F_{l-1} \times F_l}$ are the convolutional coefficients of layer l and hop k . We group all learnable coefficients $\mathcal{H} = \{\mathbf{H}_{l,k}\}_{l,k}$, and define the GNN as $\Phi(\mathbf{x}, \mathbf{S}, \mathcal{H}) = \mathbf{X}_L$.

A. Empirical Risk Minimization

We consider the problem of learning a GNN that given an input graph signal $\mathbf{x} \in \mathcal{X} \subseteq \mathbb{R}^n$ can predict an output graph signal $\mathbf{y} \in \mathcal{Y} \subseteq \mathbb{R}^n$ of an unknown distribution $p(X, Y)$,

$$\underset{\mathcal{H}}{\text{minimize}} \mathbb{E}_p[\ell(\mathbf{y}, \Phi(\mathbf{x}, \mathbf{S}, \mathcal{H}))], \quad (\text{SRM})$$

where ℓ is a non-negative loss function $\ell : \mathbb{R}^d \times \mathbb{R}^d \rightarrow \mathbb{R}^+$, such that $\ell(\mathbf{y}, \mathbf{y}) = 0$ iff $\mathbf{y} = \mathbf{y}$. Common choices for the loss function are the cross-entropy loss and the mean square error. Problem (SRM) is denoted called Statistical Risk Minimization [48], and the choice of GNN for a parameterization is justified by the structure of the data, and the invariances in the graph [3]. However, problem (SRM) cannot be solved in practice given that we do not have access to the underlying probability distribution p . In practice, we assume to be equipped with a dataset $\mathcal{D} = \{x_i, y_i\}_i$ drawn i.i.d. from the unknown probability $p(X, Y)$ with $|\mathcal{D}| = m$ samples. We can therefore obtain the empirical estimator of (SRM) as,

$$\underset{\mathcal{H}}{\text{minimize}} \mathbb{E}_{\mathcal{D}}[\ell(\mathbf{y}, \Phi(\mathbf{x}, \mathbf{S}, \mathcal{H}))] := \frac{1}{m} \sum_{i=1}^m \ell(\mathbf{y}_i, \Phi(\mathbf{x}_i, \mathbf{S}, \mathcal{H})). \quad (\text{ERM})$$

The empirical risk minimization problem (ERM) can be solved in practice given that it only requires access to a set of samples \mathcal{D} . The solution to problem (ERM) will be close to (SRM) given that the samples are i.i.d., and that there is a large number of samples m [48]. To solve problem (ERM), we will resort to gradient descent, and we will update the coefficients \mathcal{H} according to,

$$\mathcal{H}_{t+1} = \mathcal{H}_t - \eta_t \mathbb{E}_{\mathcal{D}}[\nabla_{\mathcal{H}} \ell(\mathbf{y}, f(\mathbf{x}, \mathbf{S}, \mathcal{H}))], \quad (\text{SGD})$$

where t represents the iteration, and η_t the step-size. In a centralized manner computing iteration (SGD) presents no major difficulty, and it is the usual choice of algorithm for training a GNN. When the size of the graph becomes large, and the graph data is partitioned across a set of agents, iteration (SGD) requires communication. In this paper, we consider the problem of solving the empirical risk minimization problem (ERM) through gradient descent (SGD) in a decentralized and efficient way.

III. DISTRIBUTED GNN TRAINING

Consider a set $\mathcal{Q}, |\mathcal{Q}| = Q$ of workers that jointly learn a single GNN Φ . Each machine $q \in \mathcal{Q}$ is equipped with a subset of the graph \mathbf{S} , and node data, as shown in Figure 2. Each machine is responsible for computing the features of the nodes in its local partitions for all layers in the GNN. The GNN model \mathcal{H} is replicated across all machines. To learn a GNN, we update the weights according to gradient descent (SGD), and average them across machines. This procedure is similar to the standard FedAverage algorithm used in *Federated Learning* [29].

The gradient descent iteration (SGD) cannot be computed without communication given that the data in $(\mathbf{y}, \mathbf{x})_i$ is distributed in the Q machines. To compute the gradient step (SGD), we need the machines to communicate graph data.

Algorithm 1 VARCO: Distributed Graph Training with VARiable COmmunication Rates

Split graph \mathcal{G} into Q partitions and assign them to each worker q_i , initialize the GNN with weights \mathcal{H}_0 and distribute it to all workers q_i , and fix initial compression rate c_0 , and scheduler r

repeat

Each Worker q_i : Compute the activations for each node in the local graph (cf. equation (2)) using the local nodes.

Each Worker q_i : Compress the activations of the nodes that are in the boundary using the compression mechanism (cf. equation (3)), and communicate them to the adjacent machines.

Each Worker q_i : Collect data from all adjacent machines, and compute forward pass by using non-compressed activations for local nodes and compressed activations for non-local nodes that are fetched from other machines.

Each Worker q_i : Compute parameter gradients by back-propagating errors across machines and through the differentiable compression routine. Apply the gradient step to the parameters in each worker (cf. equation (SGD)).

Server: Average parameters, send them back to workers, and update compression rate c_{t+1}

until Convergence

What we need to communicate is the data of each node in the adjacent machines; transmit the input feature x_j for each neighboring node $j \in \mathcal{N}_i^k, j \in q'$. For each node that we would like to classify, we would require all the graph data belonging to the k -hop neighborhood graph. This procedure is costly and grows with the size of the graph, which renders it unimplementable in practice.

As opposed to communicating the node features, and the graph structure for each node in the adjacent machine, we propose to communicate the features and activation of the nodes at the nodes in the boundary. Note that in this procedure the bits communicated between machines do not depend on the number of nodes in the graph and the number of features compressed can be controlled by the width of the architecture used (see Appendix A). The only computation overhead that this method requires is computing the value of the GNN at every layer for a given subset of nodes using local information only.

A. Computing the Gradient Using Remote Compressed Data

Following the framework of communicating the intermediate activation, to compute a gradient step (SGD), we require 3 communication rounds (i) the forward pass, in which each machine fetches the feature vectors of remote neighbors and propagates their messages to the nodes in the local partition, (ii) the backward pass, in which the gradients flow in the opposite direction and are accumulated in the GNN model weights, and (iii) the aggregation step in which the weight gradients are summed across all machines and used to update the GNN model weights. The communication steps for a single GNN layer are illustrated in Figure 2.

To compute a gradient step, we first compute the forward pass, for which we need the output of the GNN at a node i . To compute the output of a GNN at node i , we need to evaluate the GNN according to the graph convolution (1). Note that to evaluate (1), we require access to the value of the input features x_j for each $j \in \mathcal{N}_i^k$, which might not be on the same client as i . In this paper, we propose that the clients with nodes in \mathcal{N}_i^k , compute the forward passes *locally* (i.e. using only the nodes in their client), and communicate the compressed activations for each layer l .

Once the values of the activations are received, they are decompressed, processed by the local machine, and the output of the GNN is obtained. To obtain the gradient of the loss ℓ , the output of the GNN is compared to the true label, and the gradient with respect to the parameters of the GNN is computed. The errors are once again compressed and communicated back to the clients. Which, will update the values of the parameters of the GNN, after every client updates the values of the parameters \mathcal{H} , there is a final round of communication where the values are averaged. Note that this procedure allows the GNN to be updated using the whole graph. By controlling the number of bits communicated by the compressing-decompressing mechanism, we can control the communication overhead. Formally, the compressing and decompressing mechanism can be modeled as follows,

Definition 1. *The compression and decompression mechanism $g_{\epsilon,r}, g_{\epsilon,r}^{-1}$ with compression error ϵ , and compression rate r , satisfies that given a set of parameters $\mathbf{x} \in \mathbb{R}^n$, when compressed and decompressed, the following relation holds i.e.,*

$$\mathbf{z} = g_{\epsilon,r}(\mathbf{x}), \text{ and } \tilde{\mathbf{x}} = g_{\epsilon,r}^{-1}(g_{\epsilon,r}(\mathbf{x}))$$

$$\text{and } \mathbb{E}[\|\tilde{\mathbf{x}} - \mathbf{x}\|] \leq \delta \text{ with } \mathbb{E}[\|\tilde{\mathbf{x}} - \mathbf{x}\|^2] \leq \epsilon^2, \quad (3)$$

where $\mathbf{z} \in \mathbb{R}^{n/r}$ with $n/r \in \mathbb{Z}$ is the compressed signal. If $\delta = 0$, the compression is lossless.

Intuitively, the error ϵ , and compression rate r are related; a larger compression rate r will render a larger compression error ϵ . Also, compressed signals require less bandwidth to be communicated. Relying on the compression mechanism (3), a GNN trained using a *fixed* compression ratio r during training, will converge to a neighborhood of the optimal solution. The size of the neighborhood will be given by the variance of the compression error ϵ^2 . The first-order compression error δ is related to the mismatch in the compressed and decompressed signals. Our analysis works for any value of δ , which encompasses both lossy ($\delta > 0$), as well as loss-less compression ($\delta = 0$).

AS1. *The loss ℓ function has L Lipschitz continuous gradients, $\|\nabla \ell(\mathbf{y}_1, \mathbf{x}) - \nabla \ell(\mathbf{y}_2, \mathbf{x})\| \leq L\|\mathbf{y}_1 - \mathbf{y}_2\|$.*

AS2. *The non-linearity ρ is normalized Lipschitz.*

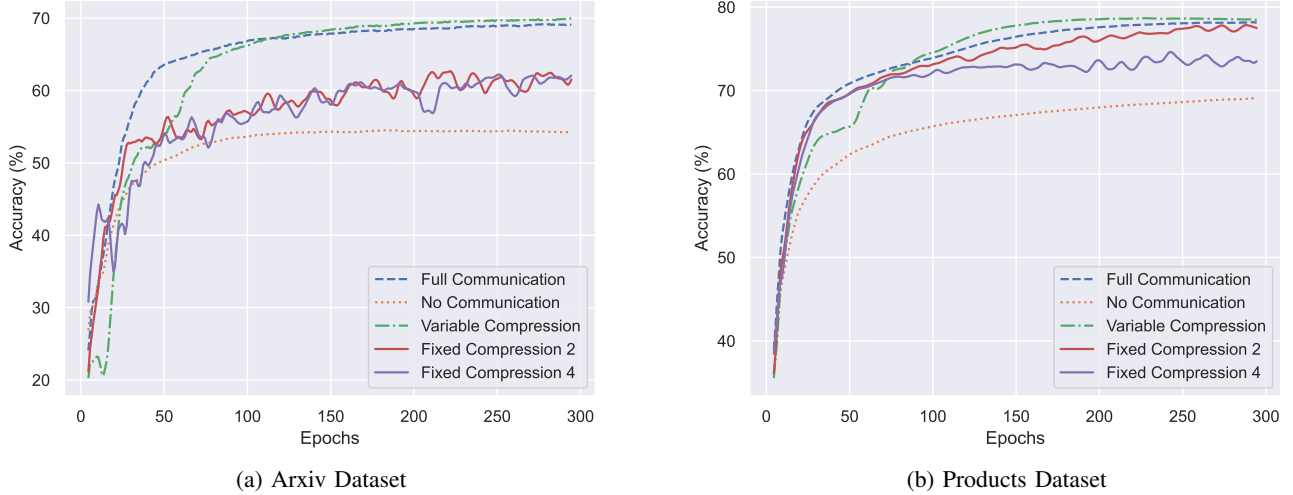


Fig. 3: Accuracy per iteration for random partitioning with 16 servers.

AS3. The GNN, and its gradients are M -Lipschitz with respect to the parameters \mathcal{H} .

AS4. The graph convolutional filters in every layer of the graph neural network are bounded, i.e.

$$\|h_* \mathbf{s} x\| \leq \|x\| \lambda_{max} \left(\sum_{t=0}^T h_t \mathbf{S}^t \right),$$

$$\text{with } \lambda_{max} \left(\sum_{t=0}^T h_t \mathbf{S}^t \right) < \infty. \quad (4)$$

Assumption 1 holds for most losses used in practice over a compact set. Assumption 2 holds for most non-linearities used in practice over normalized signals. Assumption 3 is a standard assumption, and the exact characterization is an active area of research [49]. Assumption 4 holds in practice when the weights are normalized.

Proposition 1 (Convergence of GNNs Trained on Fixed Compression). *Under assumptions 1 through 4, consider the iterates generated by equation (SGD) where the normalized signals \mathbf{x} are compressed using compression rate c with corresponding error ϵ (cf. Definition 1). Consider an L layer GNN with F , and K features and coefficients per layer respectively. Let the step-size be $\eta \leq 1/L_{\nabla}$, with $L_{\nabla} = 4M\lambda_{max}^L \sqrt{KF}$ if the compression error is such that at every step k , and any $\beta > 0$,*

$$\mathbb{E}_{\mathcal{D}} [\|\nabla_{\mathcal{H}} \ell(y, \Phi(x, \mathbf{S}; \mathcal{H}_t))\|^2] \geq L_{\nabla}^2 \epsilon^2 + \beta, \quad (5)$$

then the fixed compression mechanism converges to a neighborhood of the first-order stationary point of SRM in $K \leq \mathcal{O}(\frac{1}{\beta})$ iterations, i.e.,

$$\mathbb{E}_{\mathcal{D}} [\|\nabla_{\mathcal{H}} \ell(y, \Phi(x, \mathbf{S}; \mathcal{H}_t))\|^2] \leq L_{\nabla}^2 \epsilon^2 + \beta. \quad (6)$$

Proof. The proof can be found in Appendix C \square

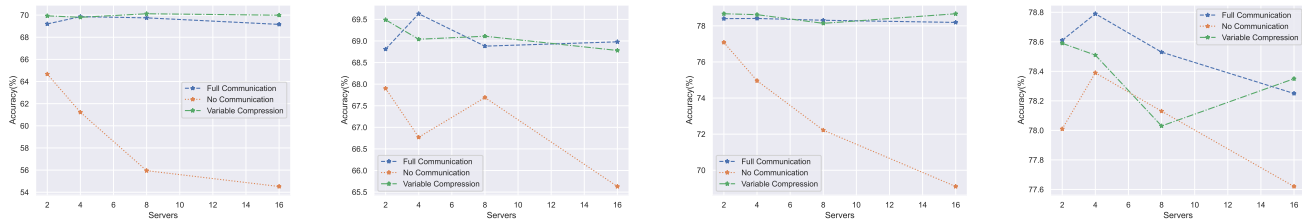
Proposition 1 is important because it allows us to show that the fixed compression mechanism can converge to a

neighborhood of the first-order stationary point of 1. The size of the neighborhood can be controlled by the compression rate ϵ . Although useful, Proposition 1, presents a limitation on the quality of the solution that can be obtained through compression. In what follows we introduce a variable compression scheme that can trade-off between efficient communication and sub-optimality guarantees.

IV. VARCO - VARIABLE COMPRESSION FOR DISTRIBUTED GNN LEARNING

In this paper, we propose variable compression rates as a way to close the gap between training in a centralized manner and efficient training in a distributed manner. We use Proposition (1) as a stepping stone towards a training mechanism that reduces the compression ratio r_t as the iterates progress. We begin by defining a scheduler $r(t) : \mathbb{Z} \rightarrow \mathbb{R}$ as a strictly decreasing function that given a train step $t \in \mathbb{Z}$, returns a compression ratio $r(t)$, such that $r(t') < r(t)$ if $t' > t$. The scheduler r will be in charge of reducing the compression ratio as the iterates increase. An example of scheduler can be the linear $r_{lin}(t) = \frac{c_{min} - c_{max}}{T} t + c_{max}$ scheduler (see Appendix 2). In this paper, we propose to train a GNN by following a compression scheme by a scheduler r , given a GNN architecture, Q -clients, and a dataset \mathcal{D} .

During the forward pass, we compute the output of the GNN at a node n_i using the local data, and the compressed data from adjacent machines. The compressed data encompasses both the features at the adjacent nodes, as well as the compressed activations of the intermediate layers for that node. The compression mechanism compresses the values of the GNN using scheduler $r(t)$, and communicates them to machine that owns node n . The backward pass receives the gradient from the machine that owns node n and updates the values of the GNN. After the GNN values are updated, the coefficients of the GNN are communicated to a centralized agent that averages them and sends them back to the machines. A more



(a) Random Part. in Arxiv Dat. (b) METIS Part. in Arxiv Dat. (c) Random Part. in Products Dat. (d) Metis Part. in Products Dat.

Fig. 4: Accuracy as a function of the number of servers.

succinct explanation of the aforementioned procedure can be found in Algorithm 1.

A. Convergence of the VARCO Algorithm

We characterize the convergence of the VARCO algorithm in the following proposition.

Proposition 2 (Scheduler Convergence). *Under assumptions 1 through 4, consider the iterates generated by equation (SGD) where the normalized signals \mathbf{x} are compressed using compression rate r with corresponding error ϵ (cf. Definition 1). Consider an L layer GNN with F , and K features and coefficients per layer respectively. Let the step-size be $\eta \leq 1/L_{\nabla}$, with $L_{\nabla} = 4M\lambda_{max}^L\sqrt{KF}$. Consider a scheduler such that the compression error ϵ_t decreases at every step $\epsilon_{t+1} < \epsilon_t$, then for any $\sigma > 0$*

$$\mathbb{E}_{\mathcal{D}}[\|\nabla_{\mathcal{H}}\ell(y, \Phi(x, \mathbf{S}; \mathcal{H}_t))\|^2] \leq \sigma. \quad (7)$$

happens infinitely often.

Proof. The proof can be found in Appendix A. \square

According to Proposition 2, for any monotonically decreasing scheduler, we can obtain an iterate t , whose gradient has a norm smaller than σ . This is an improvement to the fixed compression Proposition 1, given that we removed the term that depends on ϵ^2 , converging to a smaller neighborhood. The condition on the scheduler is simple to satisfy; the compression error $\epsilon(t)$ needs to decrease on every step (see more information about schedulers in Appendix A). This means that the scheduler does not require information about the gradient of the GNN. Compressing the activations in a GNN can prove to reduce the communication required to train it, given that the overall communication is reduced. However, keeping a fixed compression ratio might not be enough to obtain a GNN of comparable accuracy to the one trained using no compression. By using a variable compression for the communications, we obtain the best of both worlds – we reduce the communication overhead needed to train a GNN, without compromising the overall accuracy of the learned solution. The key observation is that in the early stages of training, an estimator of the gradient with a larger variance is acceptable, while in the later stages, a more precise estimator needs to be used. This behavior can be translated into efficiency; use more information from other servers only when needed.

V. EXPERIMENTS

We benchmarked our method in 2 real-world datasets: OGBN-Arxiv [50] and OGBN-Products [51]. In the case of OGBN-Arxiv, the graph has 169,343 nodes and 1,166,243 edges and it represents the citation network between computer science arXiv papers. The node features are 128 dimensional embeddings of the title and abstract of each paper [52]. The objective is to predict which of the 40 categories the paper belongs to. In the case of OGBN-Products, the graph represents products that were bought together on an online marketplace. There are 2,449,029 nodes, each of which is a product, and 61,859,140 edges which represent that the products were bought together. Feature vectors are 100 dimensional and the objective is to classify each node into 47 categories. For each dataset, we partition the graph at random and using METIS partitioning [53] and distribute it over $\{2, 4, 8, 16\}$ machines. In all cases, we trained for 300 epoch. We benchmarked VARCO against full communication, no intermediate communication, and fixed compression for $\{2, 4\}$ fixed compression ratios. For the GNNs, we used a 3 layered GNN with 256 hidden units per layer, ReLU non-linearity, and SAGE convolution [54]. For VARCO, we used a linear compression with slope 5, and 128 and 1 maximum and minimum compression ratio respectively (see Appendix A). We empirically validate the claims that we put forward, that our method (i) attains the same accuracy as the one trained with full communication without requiring a particular type of partitioning, and (ii) for the same attained accuracy, our method is more efficient in terms of communication.

A. Accuracy

We report the accuracy over the unseen data, frequently denoted test accuracy. Regarding accuracy, we can compare the performance of our variable compression algorithm VARCO, against no communication, and full communication and fixed compression ratios. In Figure 3 we present the accuracy as a function of the epoch for 16 servers and random partitions of the graph. This is the most challenging scenario given that the graph is partitioned at random and the number of partitions is the largest that we experimented with. As can be seen, our method of variable compression attains a better performance than the full communication. What is more, fixed compression has a degradation in performance in both datasets, thus validating the fact that variable compression improves upon fixed compression and no communication.

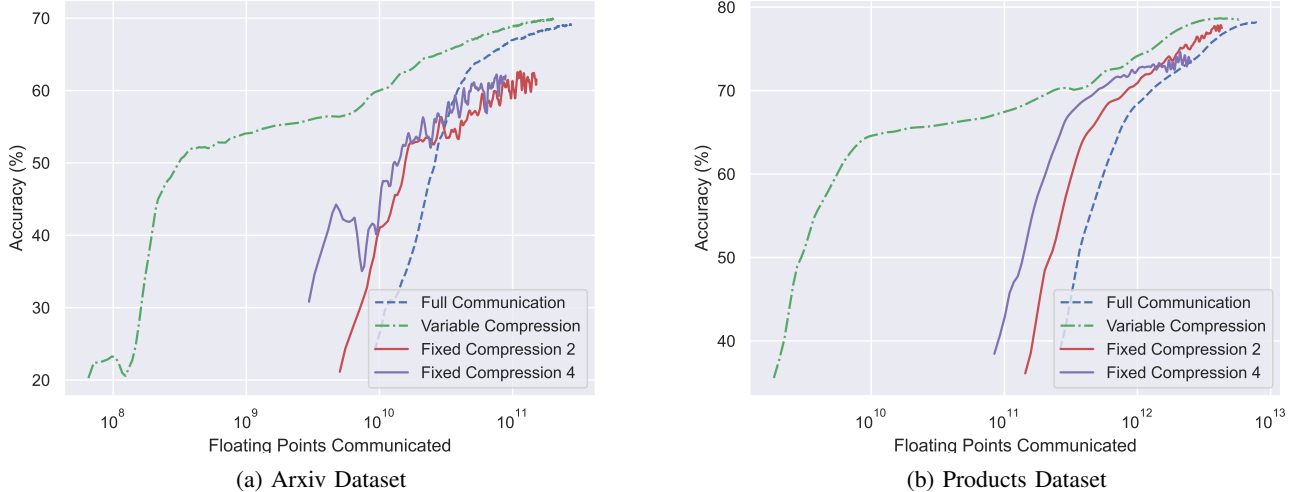


Fig. 5: Accuracy per floating points communicated for random partitioning with 16 servers.

In Figure 4 we show the accuracy as a function of the number of servers for variable compression, full communication, and no communication. We show results for both random 4a and METIS 4b partitioning for the Arxiv and Products datasets. As can be seen in all three plots, the variable compression attains a comparable performance to the one with full communication regardless of the partitioning scheme. These plots validate that our method attains a comparable performance with the one obtained with full communication both for METIS as well as random partitioning.

It is worth noting that to obtain the METIS partitioning, we need to run a min-cut algorithm which is very expensive in practice. Also, it needs to be run on a centralized computer, requiring access to the whole graph dataset. However, our algorithm does not require the graph to be partitioned in any particular way and attains the same results in random as well as METIS partitioning, as can be seen in Figures 4a, and 4c.

B. Efficiency

In terms of efficiency, we can plot the accuracy as a function of the number of floating point numbers communicated between servers. The fixed compression and full communication schemes communicate a constant number of bytes in each round of communication. This number is proportional to the cross-edges between machines, multiplied by the compression coefficient, which in the case of full communication is one. Our method is particularly useful given that at the early stages of training, fewer bytes of communication are needed, and the GNN can rely more heavily on the local data. Intuitively, all learning curves show a similar slope at the beginning of training, and they converge to different values in the later stages. In Figure 5 we corroborate that our method attains the best accuracy as a function of bytes communicated throughout the full trajectory. Given that the VARCO curve in Figure 5 is above all curves, for any communication budget i.e. number of bits, VARCO obtains the best accuracy of all methods

considered. This indeed validates our claim that using VARCO is an efficient way of training a GNN.

VI. CONCLUSION

In this paper, we presented a distributed method to train GNNs by compressing the activations and reducing the overall communications. We showed that our method converges to a neighborhood of the optimal solution, while computing gradient estimators communicating fewer bytes. Theoretically, we showed that by increasing the number of bits communicated (i.e. decreasing the compression ratio) as epochs evolve, we can decrease the loss throughout the whole training trajectory. We also showed that our method only requires the compression ratio to decrease in every epoch, without the need for any information about the process. Empirically, we benchmarked our algorithm in two real-world datasets and showed that our method obtains a GNN that attains a comparable performance to the one trained on full communication, at a fraction of the communication costs.

REFERENCES

- [1] J. Zhou, G. Cui, S. Hu, Z. Zhang, C. Yang, Z. Liu, L. Wang, C. Li, and M. Sun, "Graph neural networks: A review of methods and applications," *AI open*, vol. 1, pp. 57–81, 2020.
- [2] Z. Wu, S. Pan, F. Chen, G. Long, C. Zhang, and S. Y. Philip, "A comprehensive survey on graph neural networks," *IEEE transactions on neural networks and learning systems*, vol. 32, no. 1, pp. 4–24, 2020.
- [3] M. M. Bronstein, J. Bruna, Y. LeCun, A. Szlam, and P. Vandergheynst, "Geometric deep learning: going beyond euclidean data," *IEEE Signal Processing Magazine*, vol. 34, no. 4, pp. 18–42, 2017.
- [4] F. Gama, A. G. Marques, G. Leus, and A. Ribeiro, "Convolutional neural network architectures for signals supported on graphs," *IEEE Transactions on Signal Processing*, vol. 67, no. 4, pp. 1034–1049, 2018.
- [5] F. Gama, Q. Li, E. Tolstaya, A. Prorok, and A. Ribeiro, "Decentralized control with graph neural networks," *arXiv preprint arXiv:2012.14906*, 2020.
- [6] M. Tzes, N. Bousias, E. Chatzipantazis, and G. J. Pappas, "Graph neural networks for multi-robot active information acquisition," in *2023 IEEE International Conference on Robotics and Automation (ICRA)*. IEEE, 2023, pp. 3497–3503.

- [7] R. Lam, A. Sanchez-Gonzalez, M. Willson, P. Wirsberger, M. Fortunato, A. Pritzel, S. Ravuri, T. Ewalds, F. Alet, Z. Eaton-Rosen *et al.*, “Graphcast: Learning skillful medium-range global weather forecasting,” *arXiv preprint arXiv:2212.12794*, 2022.
- [8] J. Jumper, R. Evans, A. Pritzel, T. Green, M. Figurnov, O. Ronneberger, K. Tunyasuvunakool, R. Bates, A. Žídek, A. Potapenko *et al.*, “Highly accurate protein structure prediction with alphafold,” *Nature*, vol. 596, no. 7873, pp. 583–589, 2021.
- [9] M. Fortunato, T. Pfaff, P. Wirsberger, A. Pritzel, and P. Battaglia, “Multiscale meshgraphnets,” in *ICML 2022 2nd AI for Science Workshop*, 2022.
- [10] S. Maskey, R. Levie, Y. Lee, and G. Kutyniok, “Generalization analysis of message passing neural networks on large random graphs,” in *Advances in Neural Information Processing Systems*, S. Koyejo, S. Mohamed, A. Agarwal, D. Belgrave, K. Cho, and A. Oh, Eds., vol. 35. Curran Associates, Inc., 2022, pp. 4805–4817. [Online]. Available: https://proceedings.neurips.cc/paper_files/paper/2022/file/1eeaae7c89d9484926db6974b6ece564-Paper-Conference.pdf
- [11] Z. Wang, J. Cervino, and A. Ribeiro, “A Manifold Perspective on the Statistical Generalization of Graph Neural Networks,” *arXiv e-prints*, p. arXiv:2406.05225, Jun. 2024.
- [12] N. Keriven and G. Peyré, “Universal invariant and equivariant graph neural networks,” *Advances in Neural Information Processing Systems*, vol. 32, 2019.
- [13] V. G. Satorras, E. Hoogeboom, and M. Welling, “E (n) equivariant graph neural networks,” in *International conference on machine learning*. PMLR, 2021, pp. 9323–9332.
- [14] F. Gama, J. Bruna, and A. Ribeiro, “Stability properties of graph neural networks,” *IEEE Transactions on Signal Processing*, vol. 68, pp. 5680–5695, 2020.
- [15] L. Ruiz, L. Chamon, and A. Ribeiro, “Graphon neural networks and the transferability of graph neural networks,” *Advances in Neural Information Processing Systems*, vol. 33, pp. 1702–1712, 2020.
- [16] K. Xu, W. Hu, J. Leskovec, and S. Jegelka, “How powerful are graph neural networks?” in *International Conference on Learning Representations*, 2018.
- [17] G. Bouritsas, F. Frasca, S. Zafeiriou, and M. M. Bronstein, “Improving graph neural network expressivity via subgraph isomorphism counting,” *IEEE Transactions on Pattern Analysis and Machine Intelligence*, vol. 45, no. 1, pp. 657–668, 2022.
- [18] C. I. Kanatsoulis and A. Ribeiro, “Graph neural networks are more powerful than we think,” *arXiv preprint arXiv:2205.09801*, 2022.
- [19] Z. Chen, S. Villar, L. Chen, and J. Bruna, “On the equivalence between graph isomorphism testing and function approximation with gnns,” *arXiv preprint arXiv:1905.12560*, 2019.
- [20] S. Maskey, R. Levie, and G. Kutyniok, “Transferability of graph neural networks: an extended graphon approach,” *Applied and Computational Harmonic Analysis*, vol. 63, pp. 48–83, 2023.
- [21] J. Cerviño, L. Ruiz, and A. Ribeiro, “Learning by transference: Training graph neural networks on growing graphs,” *IEEE Transactions on Signal Processing*, vol. 71, pp. 233–247, 2023.
- [22] J. Cerviño, L. Ruiz, and A. Ribeiro, “Training graph neural networks on growing stochastic graphs,” in *ICASSP 2023 - 2023 IEEE International Conference on Acoustics, Speech and Signal Processing (ICASSP)*, 2023, pp. 1–5.
- [23] Z. Cai, X. Yan, Y. Wu, K. Ma, J. Cheng, and F. Yu, “Dgcl: an efficient communication library for distributed gnn training,” in *Proceedings of the Sixteenth European Conference on Computer Systems*, 2021, pp. 130–144.
- [24] L. Wang, Q. Yin, C. Tian, J. Yang, R. Chen, W. Yu, Z. Yao, and J. Zhou, “Flexgraph: a flexible and efficient distributed framework for gnn training,” in *Proceedings of the Sixteenth European Conference on Computer Systems*, 2021, pp. 67–82.
- [25] D. Zheng, C. Ma, M. Wang, J. Zhou, Q. Su, X. Song, Q. Gan, Z. Zhang, and G. Karypis, “Distdgl: distributed graph neural network training for billion-scale graphs,” in *2020 IEEE/ACM 10th Workshop on Irregular Applications: Architectures and Algorithms (IA3)*. IEEE, 2020, pp. 36–44.
- [26] Q. Wang, Y. Zhang, H. Wang, C. Chen, X. Zhang, and G. Yu, “Neutronstar: distributed gnn training with hybrid dependency management,” in *Proceedings of the 2022 International Conference on Management of Data*, 2022, pp. 1301–1315.
- [27] K. Bonawitz, H. Eichner, W. Grieskamp, D. Huba, A. Ingerman, V. Ivanov, C. Kiddon, J. Konečný, S. Mazzocchi, B. McMahan *et al.*, “Towards federated learning at scale: System design,” *Proceedings of machine learning and systems*, vol. 1, pp. 374–388, 2019.
- [28] L. Li, Y. Fan, M. Tse, and K.-Y. Lin, “A review of applications in federated learning,” *Computers & Industrial Engineering*, vol. 149, p. 106854, 2020.
- [29] T. Li, A. K. Sahu, A. Talwalkar, and V. Smith, “Federated learning: Challenges, methods, and future directions,” *IEEE signal processing magazine*, vol. 37, no. 3, pp. 50–60, 2020.
- [30] Z. Shen, J. Cervino, H. Hassani, and A. Ribeiro, “An agnostic approach to federated learning with class imbalance,” in *International Conference on Learning Representations*, 2022. [Online]. Available: <https://openreview.net/forum?id=Xo0lbDt975>
- [31] C. He, K. Balasubramanian, E. Ceyani, C. Yang, H. Xie, L. Sun, L. He, L. Yang, P. S. Yu, Y. Rong *et al.*, “Fedgraphnn: A federated learning system and benchmark for graph neural networks,” *arXiv preprint arXiv:2104.07145*, 2021.
- [32] G. Mei, Z. Guo, S. Liu, and L. Pan, “Sggn: A graph neural network based federated learning approach by hiding structure,” in *2019 IEEE International Conference on Big Data (Big Data)*. IEEE, 2019, pp. 2560–2568.
- [33] G. Karypis and V. Kumar, “A fast and high quality multilevel scheme for partitioning irregular graphs,” *SIAM Journal on scientific Computing*, vol. 20, no. 1, pp. 359–392, 1998.
- [34] T. Kaler, A. Iliopoulos, P. Murzynowski, T. Schardl, C. E. Leiserson, and J. Chen, “Communication-efficient graph neural networks with probabilistic neighborhood expansion analysis and caching,” *Proceedings of Machine Learning and Systems*, vol. 5, 2023.
- [35] H. Mostafa, “Sequential aggregation and rematerialization: Distributed full-batch training of graph neural networks on large graphs,” *Proceedings of Machine Learning and Systems*, vol. 4, pp. 265–275, 2022.
- [36] H. Mostafa, A. Grabowski, M. A. Turja, J. Cervino, A. Ribeiro, and N. Himayat, “Fastsample: Accelerating distributed graph neural network training for billion-scale graphs,” *arXiv preprint arXiv:2311.17847*, 2023.
- [37] V. Md, S. Misra, G. Ma, R. Mohanty, E. Georganas, A. Heinecke, D. Kalamkar, N. K. Ahmed, and S. Avancha, “Distggn: Scalable distributed training for large-scale graph neural networks,” in *Proceedings of the International Conference for High Performance Computing, Networking, Storage and Analysis*, 2021, pp. 1–14.
- [38] Y. Ma, P. Gong, J. Yi, Z. Yao, C. Li, Y. He, and F. Yan, “Bifeat: Supercharge gnn training via graph feature quantization,” *arXiv preprint arXiv:2207.14696*, 2022.
- [39] M. Bahri, G. Bahl, and S. Zafeiriou, “Binary graph neural networks,” in *Proceedings of the IEEE/CVF conference on computer vision and pattern recognition*, 2021, pp. 9492–9501.
- [40] M. Ding, K. Kong, J. Li, C. Zhu, J. Dickerson, F. Huang, and T. Goldstein, “Vq-gnn: A universal framework to scale up graph neural networks using vector quantization,” *Advances in Neural Information Processing Systems*, vol. 34, pp. 6733–6746, 2021.
- [41] B. Feng, Y. Wang, X. Li, S. Yang, X. Peng, and Y. Ding, “Sgquant: Squeezing the last bit on graph neural networks with specialized quantization,” in *2020 IEEE 32nd International Conference on Tools with Artificial Intelligence (ICTAI)*. IEEE, 2020, pp. 1044–1052.
- [42] S. A. Taylor, J. Fernandez-Marques, and N. D. Lane, “Degree-quant: Quantization-aware training for graph neural networks,” in *International Conference on Learning Representations*, 2020.
- [43] B. Wan, J. Zhao, and C. Wu, “Adaptive message quantization and parallelization for distributed full-graph gnn training,” *Proceedings of Machine Learning and Systems*, vol. 5, 2023.
- [44] H. Zeng, M. Zhang, Y. Xia, A. Srivastava, A. Malevich, R. Kannan, V. Prasanna, L. Jin, and R. Chen, “Decoupling the depth and scope of graph neural networks,” in *Advances in Neural Information Processing Systems*, M. Ranzato, A. Beygelzimer, Y. Dauphin, P. Liang, and J. W. Vaughan, Eds., vol. 34. Curran Associates, Inc., 2021, pp. 19665–19679. [Online]. Available: https://proceedings.neurips.cc/paper_files/paper/2021/file/a378383b89e6719e15cd1aa45478627c-Paper.pdf
- [45] Y. Bai, C. Li, Z. Lin, Y. Wu, Y. Miao, Y. Liu, and Y. Xu, “Efficient data loader for fast sampling-based gnn training on large graphs,” *IEEE Transactions on Parallel and Distributed Systems*, vol. 32, no. 10, pp. 2541–2556, 2021.
- [46] M. Serafini and H. Guan, “Scalable graph neural network training: The case for sampling,” *ACM SIGOPS Operating Systems Review*, vol. 55, no. 1, pp. 68–76, 2021.
- [47] Y. Liu, X. Ao, Z. Qin, J. Chi, J. Feng, H. Yang, and Q. He, “Pick and choose: a gnn-based imbalanced learning approach for fraud detection,” in *Proceedings of the web conference 2021*, 2021, pp. 3168–3177.
- [48] V. Vapnik, *The nature of statistical learning theory*. Springer science & business media, 2013.

- [49] M. Fazlyab, A. Robey, H. Hassani, M. Morari, and G. Pappas, “Efficient and accurate estimation of lipschitz constants for deep neural networks,” *Advances in Neural Information Processing Systems*, vol. 32, pp. 11 427–11 438, 2019.
- [50] K. Wang, Z. Shen, C. Huang, C.-H. Wu, Y. Dong, and A. Kanakia, “Microsoft academic graph: When experts are not enough,” *Quantitative Science Studies*, vol. 1, no. 1, pp. 396–413, 2020.
- [51] K. Bhatia, K. Dahiya, H. Jain, P. Kar, A. Mittal, Y. Prabhu, and M. Varma, “The extreme classification repository: Multi-label datasets and code,” 2016. [Online]. Available: <http://manikvarma.org/downloads/XC/XMLRepository.html>
- [52] T. Mikolov, I. Sutskever, K. Chen, G. S. Corrado, and J. Dean, “Distributed representations of words and phrases and their compositionality,” in *Advances in Neural Information Processing Systems*, C. Burges, L. Bottou, M. Welling, Z. Ghahramani, and K. Weinberger, Eds., vol. 26. Curran Associates, Inc., 2013. [Online]. Available: https://proceedings.neurips.cc/paper_files/paper/2013/file/9aa42b31882ec039965f3c4923ce901b-Paper.pdf
- [53] G. KARYPIS, “Metis, a software package for partitioning unstructured graphs, partitioning meshes, and computing fill-reducing orderings of sparse matrices version 4.0,” <http://glaros.dtc.umn.edu/gkhome/metis/metis/download>, 1997.
- [54] W. Hamilton, Z. Ying, and J. Leskovec, “Inductive representation learning on large graphs,” *Advances in neural information processing systems*, vol. 30, 2017.
- [55] D. P. Bertsekas and J. N. Tsitsiklis, “Gradient convergence in gradient methods with errors,” *SIAM Journal on Optimization*, vol. 10, no. 3, pp. 627–642, 2000.
- [56] R. Durrett, *Probability: Theory and Examples*. Cambridge University Press, 2019.

APPENDIX

For the compression mechanism, we communicate the total number of elements in the feature vector and intermediate activations divided by the compression ratio. Which values of the vectors to communicate are chosen at random at the encoder’s end. For the decoder to know which element of the vector corresponds to the true values, a random key generator is shared a priori. The decoder simply places the values communicated in the corresponding position and sets a 0 on the rest of the non-communicated values.

A. Scheduler

Several strategies can be utilized to increase the compress rate as we learn. A simple strategy is to increase it a fixed rate $r_{k+1} = r_k + R$, where R is the fixed rate. Another strategy is to implement linear increase $r_k = \alpha k + r_0$, where $\alpha > 0$ is the increasing slope. Another strategy is to implement an exponential increase $r_k = \frac{1}{\beta^{K-k+1}}$, with β being the base of the exponential increase, and K the total number of steps. In all cases, the scheduler is a monotone-increasing function.

In our experiments, we considered 6 different types of variable compression mechanisms based on the following equation,

$$c = \min \left(c_{max} - a \frac{c_{max} - c_{min}}{K} k, c_{min} \right) \quad (8)$$

We considered the slope $a = \{2, 3, 4, 5, 6, 7\}$ and in all cases $c_{max} = 128$, $c_{min} = 1$.

In all cases, the partitions had the same number of nodes in each partition. In Table I we show the number of edges in each server, and across servers. As can be seen, the number of cross edges in METIS partitioning is always smaller than

random, which makes sense given the objective of the METIS algorithm. Another important aspect is that as the number of partitions increases, the cross-partition number of edges increases and correspondingly the self-partition decreases. This is why the degradation happens, local graphs are smaller, and more communication is needed.

B. Accuracy

The variable compression mechanism recovers the no communication accuracy in all cases considered. There is no difference in the accuracy obtained with variable compression, and full communication. This is true, for all numbers of servers considered, and all partitions as can be seen in Tables II, and III for METIS and random partition respectively.

C. Proof of Proposition 1

To begin with, we need to show these three lemmas.

Lemma 1 (GNN Function Difference). *Under the assumptions of Proposition 1, the output of an L -layer GNN with F and coefficients and K filter taps per layer can be bounded by,*

$$\|\Phi(\mathbf{X}_1, \mathbf{S}; \mathcal{H}) - \Phi(\mathbf{X}_2, \mathbf{S}; \mathcal{H})\| \leq \lambda_{\max}^L \|\mathbf{X}_1 - \mathbf{X}_2\| \quad (9)$$

of Lemma 1. Starting with the first layer of the GNN, and considering a single feature $\|\mathbf{x}_{l1} - \mathbf{x}_{l2}\|$, we can look into the difference between the successive layers as follows,

$$\|\mathbf{X}_{l1} - \mathbf{X}_{l2}\| = \left\| \rho \left(\sum_{k=0}^{K-1} \mathbf{H}_k \mathbf{S}^k \mathbf{x}_{l1} \right) - \rho \left(\sum_{k=0}^{K-1} \mathbf{H}_k \mathbf{S}^k \mathbf{x}_{l2} \right) \right\| \quad (10)$$

$$\leq \left\| \sum_{k=0}^{K-1} \mathbf{H}_k \mathbf{S}^k \mathbf{X}_1 - \sum_{k=0}^{K-1} \mathbf{H}_k \mathbf{S}^k \mathbf{X}_2 \right\| \quad (11)$$

$$\leq \lambda_{\max} \|\mathbf{X}_1 - \mathbf{X}_2\| \quad (12)$$

Where (11) holds by normalized Lipschitz assumption 2, and (12) holds by the normalized filters assumption 4 By repeating the recursion over L layers we attain the desired result. \square

Lemma 2 (GNN Gradient Difference). *Under the assumptions of Proposition 1, the output of an L -layer GNN with F and coefficients and K filter taps per layer can be bounded by,*

$$\|\nabla_{\mathcal{H}} \Phi(\mathbf{X}_1, \mathbf{S}; \mathcal{H}) - \nabla_{\mathcal{H}} \Phi(\mathbf{X}_2, \mathbf{S}; \mathcal{H})\| \leq 2\lambda_{\max} \sqrt{KFL} \|\mathbf{X}_1 - \mathbf{X}_2\| \quad (13)$$

of Lemma 2. Starting with the first layer of the GNN, note that the derivative of the GNN with respect to any parameter in the first layer is the value of the polynomial. By denoting h_v an element on the first layer of the GNN, the derivative with respect to the first layer is,

$$\nabla_{h_v} \rho \left(\sum_{k=0}^{K-1} \mathbf{H}_k \mathbf{S}^k \mathbf{X}_1 \right) = \rho \left(\sum_{k=0}^{K-1} \mathbf{H}_k \mathbf{S}^k \mathbf{X}_1 \right) \mathbf{S}^k \mathbf{X}_1. \quad (14)$$

Edge Type	Partitioning	Number of Servers			
		OGBN-Products			
		2	4	8	16
Self	METIS	122019051(96.71%)	118533121(93.95%)	113962769(90.33%)	110067019(87.24%)
Self	Random	64302907(50.97%)	33378937(26.46%)	17913873(14.2%)	10179253(8.07%)
Cross	METIS	4148258(3.29%)	7634188(6.05%)	12204540(9.67%)	16100290(12.76%)
Cross	Random	61864402(49.03%)	92788372(73.54%)	108253436(85.8%)	115988056(91.93%)
		OGBN-Arxiv			
Self	METIS	2173087(87.45%)	2038291(82.03%)	1864471(75.03%)	1677943(67.52%)
Self	Random	1326581(53.38%)	749367(30.16%)	459233(18.48%)	314967(12.68%)
Cross	METIS	311854(12.55%)	446650(17.97%)	620470(24.97%)	806998(32.48%)
Cross	Random	1158360(46.62%)	1735574(69.84%)	2025708(81.52%)	2169974(87.32%)

TABLE I: Number of self-edges and cross-edges for the different settings considered.

Algorithm	OGBN-Products				OGBN-Arxiv			
	Number of Servers							
	2	4	8	16	2	4	8	16
Full Comm	78.40	78.41	78.31	78.19	69.20	69.86	69.75	69.16
No Comm	77.08	74.96	72.22	69.10	64.67	61.22	55.95	54.52
Variable Comp. Slope 2(ours)	78.28	78.32	78.13	78.20	69.21	69.30	69.89	69.80
Variable Comp. Slope 3(ours)	78.56	78.81	78.61	78.79	69.24	69.48	70.21	70.07
Variable Comp. Slope 4(ours)	78.47	78.81	78.53	78.64	69.47	69.51	69.95	69.90
Variable Comp. Slope 5(ours)	78.67	78.62	78.14	78.67	69.93	69.80	70.12	69.99
Variable Comp. Slope 6(ours)	78.71	78.66	78.56	78.55	69.49	69.59	70.09	70.02
Variable Comp. Slope 7(ours)	78.38	78.70	78.45	78.71	69.21	69.89	69.90	69.81
Fixed Comp Rate 2	78.35	78.13	78.00	77.85	66.04	64.97	64.34	62.68
Fixed Comp Rate 4	78.60	77.50	76.08	74.62	66.30	63.93	63.79	62.21

TABLE II: Accuracy results when training GNNs with full-communication, no communication, fixed and variable compression in both OGBN-Arxiv, and OGBN-Products. We test our Algorithm with 2, 4, 8 and 16 clients with **random partitioning** of the graph.

Algorithm	OGBN-Products				OGBN-Arxiv			
	Number of Servers							
	2	4	8	16	2	4	8	16
Full Comm	78.61	78.79	78.53	78.25	68.81	69.63	68.88	68.98
No Comm	78.01	78.39	78.13	77.62	67.90	66.77	67.69	65.63
Variable Comp. Slope 2(ours)	78.43	78.12	78.80	78.57	69.25	68.72	69.08	69.14
Variable Comp. Slope 3(ours)	78.50	78.26	78.21	78.31	69.89	69.48	68.86	69.58
Variable Comp. Slope 4(ours)	78.73	78.01	78.13	78.58	69.39	68.96	68.75	69.16
Variable Comp. Slope 5(ours)	78.59	78.51	78.03	78.35	69.49	69.04	69.11	68.78
Variable Comp. Slope 6(ours)	78.21	78.61	78.50	78.68	69.33	68.60	69.41	69.36
Variable Comp. Slope 7(ours)	78.32	78.39	78.36	78.56	69.24	69.28	68.12	69.05
Fixed Comp Rate 2	78.49	78.49	78.18	78.46	67.68	67.76	66.73	65.78
Fixed Comp Rate 4	78.62	78.31	78.42	78.34	67.75	66.64	66.96	66.09

TABLE III: Accuracy results when training GNNs with full-communication, no communication, fixed and variable compression in both OGBN-Arxiv, and OGBN-Products. We test our Algorithm with 2, 4, 8 and 16 clients with **METIS partitioning** of the graph.

By taking the difference we get,

$$\|\nabla_{k_v} \rho \left(\sum_{k=0}^{K-1} \mathbf{H}_k \mathbf{S}^k \mathbf{x}_1 \right) - \nabla_{k_v} \rho \left(\sum_{k=0}^{K-1} \mathbf{H}_k \mathbf{S}^k \mathbf{X}_2 \right)\| \quad (15)$$

$$= \left\| \rho \left(\sum_{k=0}^{K-1} \mathbf{H}_k \mathbf{S}^k \mathbf{X}_1 \right) \mathbf{S}^k \mathbf{X}_1 - \rho \left(\sum_{k=0}^{K-1} \mathbf{H}_k \mathbf{S}^k \mathbf{X}_2 \right) \mathbf{S}^k \mathbf{X}_2 \right\| \quad (16)$$

$$\leq \left\| \rho \left(\sum_{k=0}^{K-1} \mathbf{H}_k \mathbf{S}^k \mathbf{X}_1 \right) \left(\mathbf{S}^k \mathbf{X}_1 - \mathbf{S}^k \mathbf{X}_2 \right) \right\| \quad (17)$$

$$+ \left\| \left(\rho \left(\sum_{k=0}^{K-1} \mathbf{H}_k \mathbf{S}^k \mathbf{X}_1 \right) - \rho \left(\sum_{k=0}^{K-1} \mathbf{H}_k \mathbf{S}^k \mathbf{X}_2 \right) \right) \left(\mathbf{S}^k \mathbf{X}_2 \right) \right\| \quad (18)$$

Now, given that the activation is normalized Lipschitz by assumption 2, the signals are normalized, and that the filter is normalized by assumption 4, we can bound this term by,

$$\|\nabla_{k_v} \rho \left(\sum_{k=0}^{K-1} \mathbf{H}_k \mathbf{S}^k \mathbf{X}_1 \right) - \nabla_{k_v} \rho \left(\sum_{k=0}^{K-1} \mathbf{H}_k \mathbf{S}^k \mathbf{X}_2 \right)\| \leq 2\lambda_{\max} \|\mathbf{X}_1 - \mathbf{X}_2\| \quad (19)$$

By repeating the previous result for all layers, and all features and considering that the GNN has KFL coefficients, we complete the proof. \square

Lemma 3 (Lipschitz Gradients with respect to the parameters). *Under the assumptions of Proposition 1, the output of an L -*

layer GNN with F and coefficients and K filter taps per layer can be bounded by,

$$\begin{aligned} & \|\nabla_{\mathcal{H}}\ell(\mathbf{y}, \Phi(\mathbf{x}, \mathbf{S}; \mathcal{H}_1)) - \nabla_{\mathcal{H}}\ell(\mathbf{y}, \Phi(\mathbf{x}, \mathbf{S}; \mathcal{H}_2))\| \\ & \leq 2ML\|\mathcal{H}_1 - \mathcal{H}_2\| \end{aligned} \quad (20)$$

of Lemma 3. We begin by using the chain rule as follows,

$$\|\nabla_{\mathcal{H}}\ell(\mathbf{y}, \Phi(\mathbf{x}, \mathbf{S}; \mathcal{H}_1)) - \nabla_{\mathcal{H}}\ell(\mathbf{y}, \Phi(\mathbf{x}, \mathbf{S}; \mathcal{H}_2))\| \quad (21)$$

$$\begin{aligned} & = \|\nabla\ell(\mathbf{y}, \Phi(\mathbf{x}, \mathbf{S}; \mathcal{H}_1))\nabla_{\mathcal{H}}\Phi(\mathbf{x}, \mathbf{S}; \mathcal{H}_1) \\ & - \nabla\ell(\mathbf{y}, \Phi(\mathbf{x}, \mathbf{S}; \mathcal{H}_2))\nabla_{\mathcal{H}}\Phi(\mathbf{x}, \mathbf{S}; \mathcal{H}_2)\| \end{aligned} \quad (22)$$

$$\begin{aligned} & \leq \left\| \left(\nabla\ell(\mathbf{y}, \Phi(\mathbf{x}, \mathbf{S}; \mathcal{H}_1)) \right. \right. \\ & \left. \left. - \nabla\ell(\mathbf{y}, \Phi(\mathbf{x}, \mathbf{S}; \mathcal{H}_2)) \right) \nabla_{\mathcal{H}}\Phi(\mathbf{x}, \mathbf{S}; \mathcal{H}_2) \right\| \end{aligned} \quad (23)$$

$$\begin{aligned} & + \left\| \left(\nabla_{\mathcal{H}}\Phi(\mathbf{x}_1, \mathbf{S}; \mathcal{H}) - \nabla_{\mathcal{H}}\Phi(\mathbf{x}, \mathbf{S}; \mathcal{H}_2) \right) \right. \\ & \left. \nabla\ell(\mathbf{y}, \Phi(\mathbf{x}, \mathbf{S}; \mathcal{H}_1)) \right\| \end{aligned} \quad (24)$$

Note that we consider the filters \mathcal{H} as a vector, where the coefficients have been concatenated. We can now use Cauchy-Schwartz to obtain,

$$\|\nabla_{\mathcal{H}}\ell(\mathbf{y}, \Phi(\mathbf{x}, \mathbf{S}; \mathcal{H}_1)) - \nabla_{\mathcal{H}}\ell(\mathbf{y}, \Phi(\mathbf{x}, \mathbf{S}; \mathcal{H}_2))\| \quad (25)$$

$$\begin{aligned} & \leq \|\nabla\ell(\mathbf{y}, \Phi(\mathbf{x}, \mathbf{S}; \mathcal{H}_1)) - \nabla\ell(\mathbf{y}, \Phi(\mathbf{x}, \mathbf{S}; \mathcal{H}_2))\| \\ & \|\nabla_{\mathcal{H}}\Phi(\mathbf{x}, \mathbf{S}; \mathcal{H}_2)\| \end{aligned} \quad (26)$$

$$\begin{aligned} & + \|\nabla_{\mathcal{H}}\Phi(\mathbf{x}, \mathbf{S}; \mathcal{H}_1) - \nabla_{\mathcal{H}}\Phi(\mathbf{x}, \mathbf{S}; \mathcal{H}_2)\| \\ & \|\nabla\ell(\mathbf{y}, \Phi(\mathbf{x}, \mathbf{S}; \mathcal{H}_1))\|. \end{aligned} \quad (27)$$

We can now use Assumptions 1, and 3, to obtain

$$\begin{aligned} & \|\nabla_{\mathcal{H}}\ell(\mathbf{y}, \Phi(\mathbf{x}, \mathbf{S}; \mathcal{H}_1)) - \nabla_{\mathcal{H}}\ell(\mathbf{y}, \Phi(\mathbf{x}, \mathbf{S}; \mathcal{H}_2))\| \\ & \leq 2ML\|\mathcal{H}_1 - \mathcal{H}_2\| \end{aligned} \quad (28)$$

By denoting $L_{\nabla} = 2ML$ we complete the proof. \square

Lemma 4 (Submartingale). *Consider the iterates generated by equation SGD where the input vector \mathbf{x} is compressed with error ϵ (cf. Definition 3). Let the step-size be $\eta \leq 1/L_{\nabla}$, if the compression error is such that,*

$$\mathbb{E}_{\mathcal{D}}[\|\nabla_{\mathcal{H}}\ell(\mathbf{y}, \Phi(\mathbf{x}, \mathbf{S}; \mathcal{H}_t))\|^2] \geq L_{\nabla}^2\epsilon^2 \quad (29)$$

then the iterates satisfy that,

$$\mathbb{E}[\ell(\mathbf{y}, \Phi(\mathbf{x}, \mathbf{S}; \mathcal{H}_{t+1}))] \leq \mathbb{E}[\ell(\mathbf{y}, \Phi(\mathbf{x}, \mathbf{S}; \mathcal{H}_t))] \quad (30)$$

of Lemma 4. This proof follows the lines of [55], and we start by defining a continuous function $g(\alpha)$ as follows,

$$g(\alpha) = \mathbb{E}[\ell(\mathbf{y}, \Phi(\mathbf{x}, \mathbf{S}; \mathcal{H}_t - \alpha\eta_t\nabla\ell(\mathbf{y}, \Phi(\tilde{\mathbf{x}}, \mathbf{S}; \mathcal{H}_t)))). \quad (31)$$

Note that, $g(0) = \mathbb{E}[\ell(\mathbf{y}, \Phi(\mathbf{x}, \mathbf{S}; \mathcal{H}_t))]$ and

$g(1) = \mathbb{E}[\ell(\mathbf{y}, \Phi(\mathbf{x}, \mathbf{S}; \mathcal{H}_{k+1}))]$, and also that the integral of $\frac{\partial}{\partial\alpha}g(\alpha)$ satisfies

$$\begin{aligned} & g(1) - g(0) \\ & = \int_0^1 \frac{\partial}{\partial\alpha}g(\alpha)d\alpha \end{aligned} \quad (32)$$

$$\begin{aligned} & = -\mathbb{E}[\eta\nabla_{\mathcal{H}}\ell(\mathbf{y}, \Phi(\tilde{\mathbf{x}}, \mathbf{S}; \mathcal{H}_t))^{\top} \int_0^1 \nabla_{\mathcal{H}}\ell(\mathbf{y}, \Phi(\mathbf{x}, \mathbf{S}; \mathcal{H}_t \\ & - \alpha\eta\nabla_{\mathcal{H}}\ell(\mathbf{y}, \Phi(\tilde{\mathbf{x}}, \mathbf{S}; \mathcal{H}_t)))d\alpha] \end{aligned} \quad (33)$$

$$\begin{aligned} & = -\mathbb{E}[\eta\nabla_{\mathcal{H}}\ell(\mathbf{y}, \Phi(\tilde{\mathbf{x}}, \mathbf{S}; \mathcal{H}_t))^{\top} \int_0^1 \nabla_{\mathcal{H}}\ell(\mathbf{y}, \Phi(\mathbf{x}, \mathbf{S}; \mathcal{H}_t \\ & - \alpha\eta\nabla_{\mathcal{H}}\ell(\mathbf{y}, \Phi(\tilde{\mathbf{x}}, \mathbf{S}; \mathcal{H}_t))) \end{aligned} \quad (34)$$

$$+ \nabla_{\mathcal{H}}\ell(\mathbf{y}, \Phi(\mathbf{x}, \mathbf{S}; \mathcal{H}_t)) - \nabla_{\mathcal{H}}\ell(\mathbf{y}, \Phi(\mathbf{x}, \mathbf{S}; \mathcal{H}_t))d\alpha] \quad (35)$$

$$\begin{aligned} & = -\mathbb{E}[\eta\nabla_{\mathcal{H}}\ell(\mathbf{y}, \Phi(\tilde{\mathbf{x}}, \mathbf{S}; \mathcal{H}_t))^{\top} \nabla_{\mathcal{H}}\ell(\mathbf{y}, \Phi(\mathbf{x}, \mathbf{S}; \mathcal{H}_t)) \\ & + \eta\nabla_{\mathcal{H}}\ell(\mathbf{y}, \Phi(\tilde{\mathbf{x}}, \mathbf{S}; \mathcal{H}_t))^{\top} \int_0^1 \nabla_{\mathcal{H}}\ell(\mathbf{y}, \Phi(\mathbf{x}, \mathbf{S}; \mathcal{H}_t \\ & - \alpha\eta\nabla_{\mathcal{H}}\ell(\mathbf{y}, \Phi(\tilde{\mathbf{x}}, \mathbf{S}; \mathcal{H}_t))) \\ & - \nabla_{\mathcal{H}}\ell(\mathbf{y}, \Phi(\mathbf{x}, \mathbf{S}; \mathcal{H}_t))d\alpha], \end{aligned} \quad (36)$$

where (33) holds by the chain rule, (35) holds as we are adding and subtracting the same term, and (36) is a rearrangement of terms. We can now utilize Cauchy-Schwartz to bound the difference as follows,

$$\begin{aligned} & \mathbb{E}_{\mathcal{D}}[\ell(\mathbf{y}, \Phi(\mathbf{x}, \mathbf{S}; \mathcal{H}_{k+1})) - \ell(\mathbf{y}, \Phi(\mathbf{x}, \mathbf{S}; \mathcal{H}_t))] \\ & \leq -\mathbb{E}[\eta\nabla_{\mathcal{H}}\ell(\mathbf{y}, \Phi(\tilde{\mathbf{x}}, \mathbf{S}; \mathcal{H}_t))^{\top} \nabla_{\mathcal{H}}\ell(\mathbf{y}, \Phi(\mathbf{x}, \mathbf{S}; \mathcal{H}_t))] \quad (37) \\ & + \frac{\eta}{2}\|\nabla_{\mathcal{H}}\ell(\mathbf{y}, \Phi(\tilde{\mathbf{x}}, \mathbf{S}; \mathcal{H}_t))\|\|\nabla_{\mathcal{H}}\ell(\mathbf{y}, \Phi(\mathbf{x}, \mathbf{S}; \mathcal{H}_t \\ & - \eta\nabla_{\mathcal{H}}\ell(\mathbf{y}, \Phi(\tilde{\mathbf{x}}, \mathbf{S}; \mathcal{H}_t))) \\ & - \nabla_{\mathcal{H}}\ell(\mathbf{y}, \Phi(\mathbf{x}, \mathbf{S}; \mathcal{H}_t))\|. \end{aligned}$$

where the previous inequality holds given that $\int_0^1 \alpha^2 d\alpha = \frac{1}{2}$. We can utilize Lemma 3 to bound the difference between the gradients as follows,

$$\begin{aligned} & \mathbb{E}[\ell(\mathbf{y}, \Phi(\mathbf{x}, \mathbf{S}; \mathcal{H}_{k+1})) - \ell(\mathbf{y}, \Phi(\mathbf{x}, \mathbf{S}; \mathcal{H}_t))] \quad (38) \\ & \leq \mathbb{E}[-\eta\nabla_{\mathcal{H}}\ell(\mathbf{y}, \Phi(\tilde{\mathbf{x}}, \mathbf{S}; \mathcal{H}_t))^{\top} \nabla_{\mathcal{H}}\ell(\mathbf{y}, \Phi(\mathbf{x}, \mathbf{S}; \mathcal{H}_t)) \\ & + \frac{L_{\nabla}\eta^2}{2}\|\nabla_{\mathcal{H}}\ell(\mathbf{y}, \Phi(\tilde{\mathbf{x}}, \mathbf{S}; \mathcal{H}_t))\|^2]. \end{aligned}$$

Now, we can factor $-\eta/2$, and we obtain,

$$\begin{aligned} & \mathbb{E}[\ell(\mathbf{y}, \Phi(\mathbf{x}, \mathbf{S}; \mathcal{H}_{k+1})) - \ell(\mathbf{y}, \Phi(\mathbf{x}, \mathbf{S}; \mathcal{H}_t))] \quad (39) \\ & \leq \frac{-\eta}{2}\mathbb{E}[2\nabla_{\mathcal{H}}\ell(\mathbf{y}, \Phi(\tilde{\mathbf{x}}, \mathbf{S}; \mathcal{H}_t))^{\top} \nabla_{\mathcal{H}}\ell(\mathbf{y}, \Phi(\mathbf{x}, \mathbf{S}; \mathcal{H}_t)) \\ & - \|\nabla_{\mathcal{H}}\ell(\mathbf{y}, \Phi(\tilde{\mathbf{x}}, \mathbf{S}; \mathcal{H}_t))\|^2] \quad (40) \\ & + \mathbb{E}[\frac{L_{\nabla}\eta^2 - \eta}{2}\|\nabla_{\mathcal{H}}\ell(\mathbf{y}, \Phi(\tilde{\mathbf{x}}, \mathbf{S}; \mathcal{H}_t))\|^2]. \end{aligned}$$

Now by imposing the condition that $\eta < \frac{1}{L_{\nabla}}$, the second term can be ignored. Knowing that for any two vectors, \mathbf{a}, \mathbf{b} , $\|\mathbf{a} - \mathbf{b}\|^2 - \|\mathbf{b}\|^2 = \|\mathbf{a}\|^2 - 2\mathbf{a}^{\top}\mathbf{b}$ given that the norm is induced by the inner product we obtain,

$$\begin{aligned} & \mathbb{E}[\ell(\mathbf{y}, \Phi(\mathbf{x}, \mathbf{S}; \mathcal{H}_{k+1})) - \ell(\mathbf{y}, \Phi(\mathbf{x}, \mathbf{S}; \mathcal{H}_t))] \\ & \leq \frac{-\eta}{2}\mathbb{E}[\|\nabla_{\mathcal{H}}\ell(\mathbf{y}, \Phi(\mathbf{x}, \mathbf{S}; \mathcal{H}_t))\|^2 \\ & - \|\nabla_{\mathcal{H}}\ell(\mathbf{y}, \Phi(\tilde{\mathbf{x}}, \mathbf{S}; \mathcal{H}_t)) - \nabla_{\mathcal{H}}\ell(\mathbf{y}, \Phi(\mathbf{x}, \mathbf{S}; \mathcal{H}_t))\|^2]. \end{aligned}$$

Finally, by Lemma 2, and compression mechanism 1,

$$\begin{aligned} & \mathbb{E}[\ell(\mathbf{y}, \Phi(\mathbf{x}, \mathbf{S}; \mathcal{H}_{k+1})) - \ell(\mathbf{y}, \Phi(\mathbf{x}, \mathbf{S}; \mathcal{H}_t))] \quad (41) \\ & \leq \frac{-\eta}{2} \left(\mathbb{E}[|\nabla_{\mathcal{H}} \ell(\mathbf{y}, \Phi(\mathbf{x}, \mathbf{S}; \mathcal{H}_t))|^2] - L_{\nabla}^2 \epsilon^2 \right). \end{aligned}$$

By imposing the condition in 29 we complete the proof. \square

of Proposition 1. To begin with, for every β we define the stopping time K as

$$K = \min_{k \geq 0} \{ \mathbb{E}[|\nabla_{\mathcal{H}} \ell(\mathbf{y}, \Phi(\mathbf{x}, \mathbf{S}; \mathcal{H}_k))|^2] \leq L_{\nabla}^2 \epsilon_k^2 + \beta^2 \} \quad (42)$$

We need to show that $\mathbb{E}[k^*]$ is of order $\mathcal{O}(1/\beta)$. To do so, we start by taking the difference between the last iterate K and the first one as follows,

$$\begin{aligned} & \mathbb{E}[\ell(\mathbf{y}, \Phi(\mathbf{x}, \mathbf{S}; \mathcal{H}_0)) - \ell(\mathbf{y}, \Phi(\mathbf{x}, \mathbf{S}; \mathcal{H}_t))] \quad (43) \\ & = \mathbb{E}_K \left[\mathbb{E} \left[\sum_{k=1}^K \ell(\mathbf{y}, \Phi(\mathbf{x}, \mathbf{S}; \mathcal{H}_{k-1})) - \ell(\mathbf{y}, \Phi(\mathbf{x}, \mathbf{S}; \mathcal{H}_t)) \right] \right] \quad (44) \end{aligned}$$

$$\begin{aligned} & = \sum_{t=0}^{\infty} \mathbb{E} \left[\sum_{k=1}^t \ell(\mathbf{y}, \Phi(\mathbf{x}, \mathbf{S}; \mathcal{H}_{k-1})) \right. \\ & \left. - \ell(\mathbf{y}, \Phi(\mathbf{x}, \mathbf{S}; \mathcal{H}_t)) \right] P(K = t) \quad (45) \end{aligned}$$

Now, we know that for all $t \leq K$, we have that,

$$\mathbb{E} \left[\sum_{k=1}^K \ell(\mathbf{y}, \Phi(\mathbf{x}, \mathbf{S}; \mathcal{H}_{k-1})) - \ell(\mathbf{y}, \Phi(\mathbf{x}, \mathbf{S}; \mathcal{H}_t)) \right] \geq \eta \beta. \quad (46)$$

We can now substitute condition 46 into equation 45 to obtain,

$$\begin{aligned} & \mathbb{E}[\ell(\mathbf{y}, \Phi(\mathbf{x}, \mathbf{S}; \mathcal{H}_0)) - \ell(\mathbf{y}, \Phi(\mathbf{x}, \mathbf{S}; \mathcal{H}_t))] \quad (47) \\ & \geq \sum_{t=0}^{\infty} \eta \beta K P(K = t) \geq \beta \eta \mathbb{E}[K]. \quad (48) \end{aligned}$$

Given that the loss function is non-negative, and dividing in both sides of the previous inequality by $\beta \eta$, we complete the proof. \square

The sketch of this proof is as follows, first, we construct a martingale by multiplying the norm of the gradient by the condition that we want to satisfy. Second, we show that this construction is effectively a martingale. Third, we show that it converges. Finally, we show what the limit of this convergent martingale is.

To begin with, we define the filtration \mathcal{F}_t by iterates generated according to (SGD), and the sequence X_t as follows,

$$\begin{aligned} X_t & = \|\nabla_{\mathcal{H}} \ell(\mathbf{y}, \phi(x, \mathbf{S}; \mathcal{H}_t))\|^2 \mathbf{1}[\|\nabla_{\mathcal{H}} \ell(\mathbf{y}, \phi(x, \mathbf{S}; \mathcal{H}_t))\|^2 \\ & \geq L_{\nabla}^2 \epsilon_t^2 + \sigma, t' \leq t], \quad (49) \end{aligned}$$

where $\mathbf{1}[\cdot]$ is the indicator function. The expected value of $|X_t|$ is bounded by Assumption 1, and X_t is adapted to the filtration generated by the iterates of SGD. By [56], to show that X_n is a super-martingale, we require,

$$\mathbb{E}[X_{t+1} | \mathcal{F}_t] \leq X_t. \quad (50)$$

By contradiction, we can argue that $\mathbb{E}[X_{t+1} | \mathcal{F}_t] > X_t$. Now, if $\mathbb{E}[X_{t+1} | \mathcal{F}_t] > X_t$ for every $t > t_0$, then it must be the case

that $X_{t_0} > L_{\nabla}^2 \epsilon_{t_0}^2 + \sigma$. If this is not the case, the indicator function will make the sequence equal to 0 for all $t > t_0$, disproving the contradiction. Given that $X_{t_0} > L_{\nabla}^2 \epsilon_{t'}^2 + \sigma$, we can fix ϵ_0 , and by Proposition 1, we arrive at a contradiction, and therefore X_n is a super-martingale.

Given that the X_t is bounded below by 0, by the Martingale Convergence Theorem [56, Theorem 4.2.1], X_t converges.

Now it remains to show that the limit of $\lim_{t \rightarrow \infty} X_t = 0$. We can assume that this is not true. We can therefore assume that $\lim_{t \rightarrow \infty} X_t = A < \infty$ with $A > \sigma$. Now, we know that the scheduler decreases, and therefore $\exists t^* : L_{\nabla}^2 \epsilon_{t^*}^2 + \sigma < A$. In this case again, X_t cannot be larger than $L_{\nabla}^2 \epsilon_{t^*}^2 + \sigma$ forever by Proposition 1. Therefore, there is no $A > \sigma$ such that X_t converges to. Which implies that $X_n \rightarrow 0$.

To finalize, given that we made no assumptions over the initial time t , $\|\nabla_{\mathcal{H}} \ell(\mathbf{y}, \phi(x, \mathbf{S}; \mathcal{H}_t))\|^2 \leq \sigma$ happens infinitely often, completing the proof.